Electronic Supplementary Information

Selective upgrading of ethanol with methanol in water for the production of improved biofuel — isobutanol

Qiang Liu,[a,b,‡] Guoqiang Xu,*[a,‡] Xicheng Wang[a] and Xindong Mu*[a]

[a]CAS Key Laboratory of Bio-based Materials, Qingdao Institute of Bioenergy and Bioprocess Technology, Chinese Academy of Sciences, Qingdao, Shandong, 266101, PR China.

[b]University of Chinese Academy of Sciences, Beijing 100049, PR China.

[‡]These authors contributed equally to this work.

*Correspondence to:

E-mail: xugq@qibebt.ac.cn.

E-mail: muxd@qibebt.ac.cn.

Contents

Preparation and characterization of N functionalized carbon supports

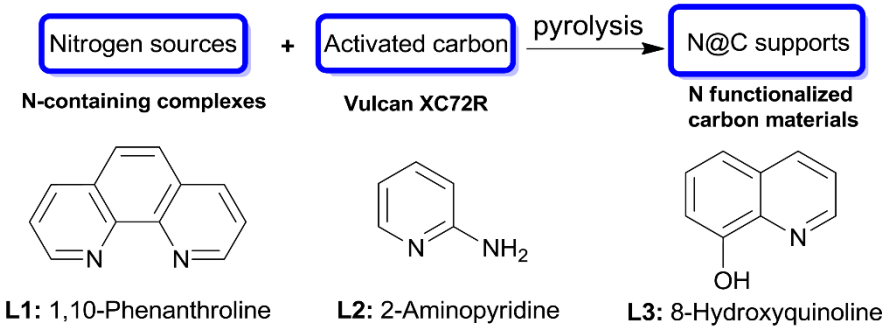

Figure S1. Schematic representation of the preparation of N functionalized carbon supports.

Protic salts of N complexes

L1-H_2SO_4

In a 250 mL round-bottom flask, 5.0 g of 1,10-phenanthroline monohydrate (L1, 25 mmol) was dissolved in 25 mL of ethanol, and then 5 g 98% H_2SO_4 (50 mmol) diluted with 25 mL of deionized water was added slowly under magnetic stirring. The mixture was stirred at room temperature for 4 hours. Phenanthroline sulfuric acid salt (L1-H_2SO_4, 9.28 g, 98.3% yield) was obtained as light yellow solid after the evaporation of ethanol and water.

L1-HCl

In a 250 mL round-bottom flask, 5.0 g of 1,10-phenanthroline monohydrate (L1, 25 mmol) was dissolved in 25 mL of ethanol, then 5 mL of a 10 M HCl diluted with 25 mL of deionized water was added slowly under magnetic stirring. The mixture was stirred at room temperature for 4 hours. Phenanthroline hydrochloric acid salt (L1-HCl, 4.98 g, 78.1% yield) was obtained as light yellow solid after the evaporation of ethanol and water.

L2-H_2SO_4

In a 250 mL round-bottom flask, 4.7 g of 2-aminopyridine (L2, 50 mmol) was dissolved in 25 mL of ethanol, and then 5 g 98% H_2SO_4 (50 mmol) diluted with 25 mL of deionized water was added slowly under magnetic stirring. After 4 hours stirring at room temperature, the mixture was evaporated to remove ethanol and water. 2-Aminopyridine sulfuric acid salt (L2-

H_2SO_4, 9.41 g, 98.0% yield) was obtained as brown solid.

L3-H_2SO_4

In a 250 mL round-bottom flask, 3.6 g of 8-hydroxyquinoline (L3, 25 mmol) was dissolved in 20 mL of ethanol, and then 2.5 g 98% H_2SO_4 (25 mmol) diluted with 25 mL of deionized water was added slowly under magnetic stirring. The mixture was stirred at room temperature for 4 hours, 8-hydroxyquinoline sulfuric acid salt (L3-H_2SO_4, 5.9 g, 97.5% yield) was obtained as yellow solid after evaporation of ethanol and water.

N functionalized carbon supports

According to reference 27, carbonaceous yield = (oven yield)/(theoretical yield). While, oven yield = (overall mass after pyrolysis - mass of activated carbon)/(mass of nitrogen source), and theoretical yield = carbon content in the nitrogen source.

Table S1. Preparation and properties of N functionalized carbon supports.

Support	N source	N source :AC (mass ratio)	T (^oC)	Yield (%)	N content (%)	Surface composition	S_{BET} (m^2/g)
S1	L1-H_2SO_4	0.5:1	700	61	1.1	N-2.7 C-94.4 O-1.5 S-1.4	125
S2	L1-H_2SO_4	1:1	700	87	2.9	N-5.6 C-91.3 O-2.4 S-0.6	113
S3	L1-H_2SO_4	2:1	700	95	4.8	N-7.1 C-87.7 O-4.6 S-0.6	128
S4	L1-H_2SO_4	0.5:1	800	62	1.0	N-2.2 C-95.5 O-1.5 S-0.8	142
S5	L1-H_2SO_4	1:1	800	86	2.2	N-4.9 C-92.1 O-2.2 S-0.7	134
S6	L1-H_2SO_4	0.5:1	900	56	0.9	N-1.4 C-96.2 O-1.4 S-1.0	175
S7	L1-H_2SO_4	1:1	900	69	1.5	N-2.9 C-92.9 O-2.8 S-1.4	138
S8	L1-HCl	2:1	900	9	1.2	N-1.3 C-97.6 O-1.0 Cl-0.1	118
S9	L2-H_2SO_4	1:1	900	39	1.2	N-2.6 C-96.0 O-0.7 S-0.7	170
S10	L2-H_2SO_4	0.5:1	900	33	0.8	N-1.6 C-95.5 O-1.2 S-1.7	210
S11	L3-H_2SO_4	1:1	900	59	1.2	N-1.5 C-93.9 O-3.1 S-1.5	104
S12	L1-H_2SO_4	no AC	900	98	/	/	6

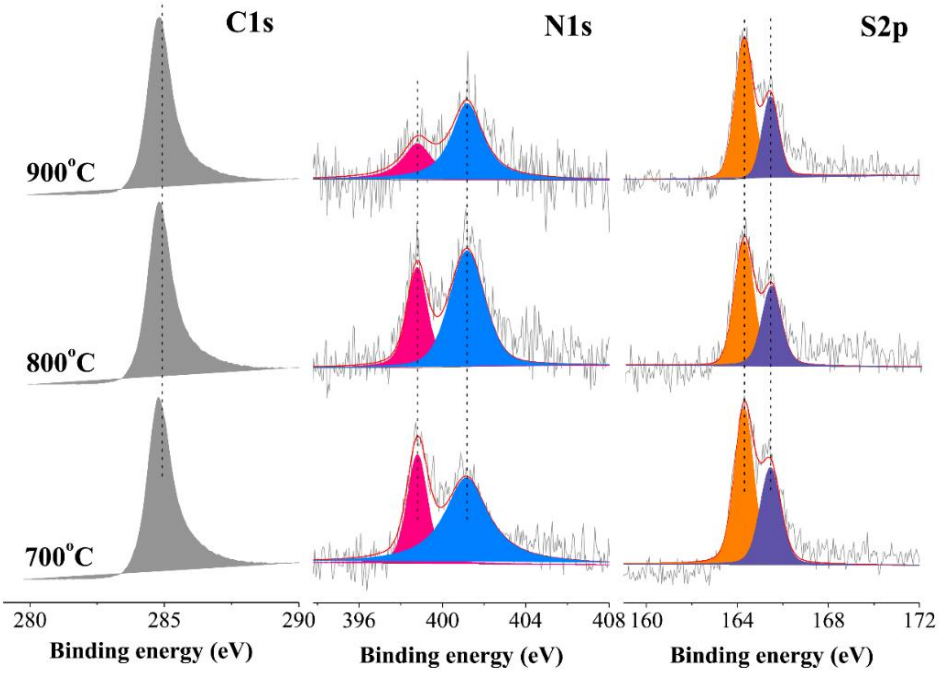

Figure S2. XPS spectra of the C, N, S of supports S1, S4 and S6 in Table S1.

Experimental results indicated the unique property of sulfuric acid in improving the carbonaceous yield (Table S1, support S8), which was similar to the previous report.[27] The ratio of N-containing salt to activated carbon and the pyrolysis temperature were important to control N content and its chemical environment in the supports. As the calcination temperature increased, total N content decreased gradually (Table S1, supports S1, S4 and S6). Peaks with binding energy (BE) of 398.7 eV and 401.1 eV correspond to pyridinic and graphitic type N, respectively. The ratio graphitic N to pyridinic N varied from 1.9:1 to 2.1:1 (Figure S2). Without activated carbon as additional carbon source, phenanthroline sulfuric acid salt (L1-H_2SO_4) generated carbonaceous material with very limited specific surface area after pyrolysis (Table S1, support S12).[27] Compared to pure carbon (Table S2), although the BET surface area decreased slightly, N-functionalized carbon support had a larger average pore diameter (BJH method).[28]

Catalyst immobilization and characterization

$Ir(acac)_3$-Phen/AC catalyst was prepared according to our previous report[18] and the content of Ir is 5 wt%, too.

Commercial Ir/C (5 wt%) was also oxidized at 250 °C for 8 hours under air before applied into the catalytic reactions (abbreviated as Ir/C (5%-250)).

Considering the slight decomposition of catalyst in air above 300 °C (Figure S3), a modified oxidation treatment (first calcined under N_2 atmosphere and then oxidized at 250 °C in air) was used for comparison.

Table S2. Surface area and pore diameter of pure carbon, N-functionalized carbon support and immobilized Ir catalyst.

Sample	BET surface area (m^2/g)	BJH adsorption average pore diameter (4V/A) (nm)
Vulcan XC-72R	222	11.8
S6 (L1-H_2SO_4, 0.5:1, 900)	175	22.2
$IrCl_3$/S6 (5%-250)	170	21.5

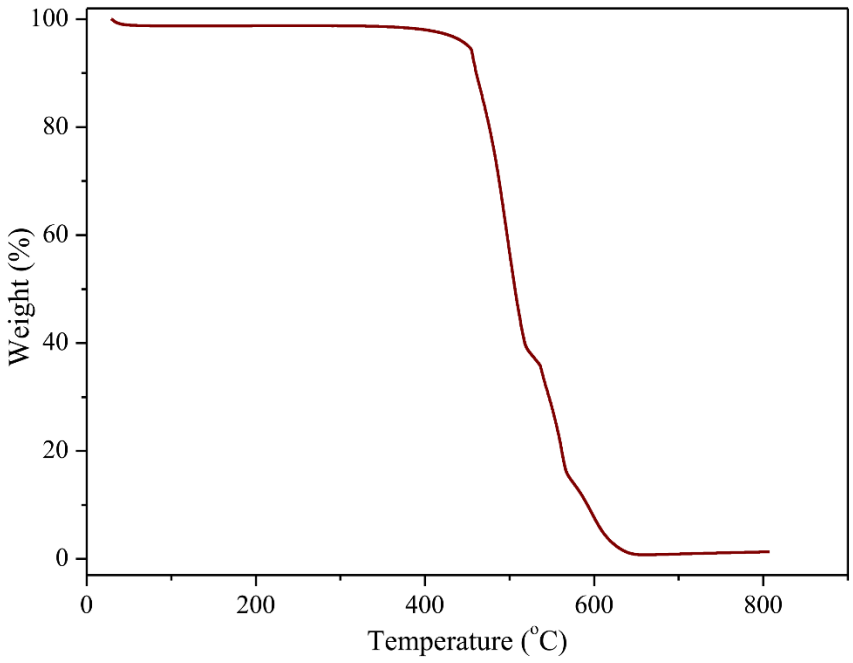

Figure S3. TG curve of $IrCl_3$/S6 (5%-105) catalyst.

Table S3. CO pulse chemisorption results of Ir catalysts.

Catalyst	CO uptake (mmol/g)	Ir dispersion (%)
$IrCl_3$/S6 (5%-105)	0.073	28.1
$IrCl_3$/S6 (5%-250)	0.065	25.0
$IrCl_3$/S0 (5%-250)	0.039	15.0

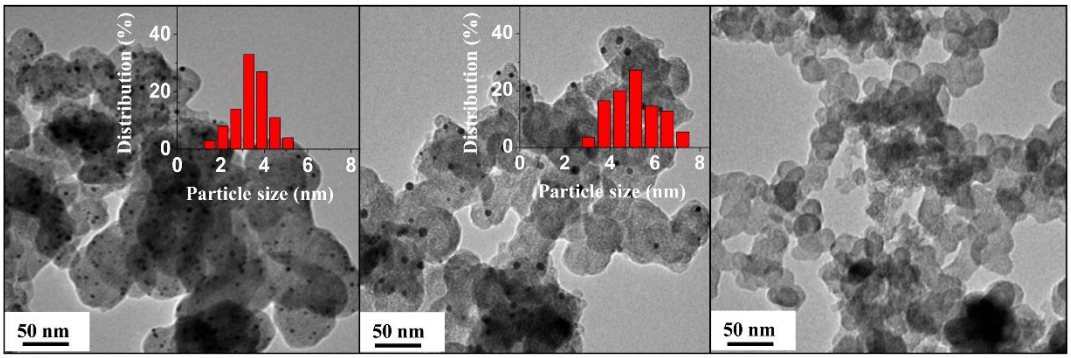

Figure S4. TEM images of $IrCl_3$/S6 (5%-300) (left); $IrCl_3$/S6 (5%-400) (middle); $IrCl_3$/S6 (5%-250) (right). Scale bar: 50 nm.

BET specific surface areas of N-functionalized carbon support and immobilized Ir catalyst decreased a little compared to Vulcan XC-72R, but the average pore diameter (BJH method) were larger (Table S2). Ir particles of the immobilized catalysts aggregated gradually above 300 ^{o}C. Within 250 ^{o}C, Ir dispersed well as very small Ir particles (< 2 nm) (Figure S4). The dispersion of Ir on N-functionalized support S6 was better than un-functionalized support S0 as evidenced from CO pulse chemisorption (Table S3).

Catalytic reactions of pure methanol and ethanol mixture

Figure 2a in the article was obtained based on entries 1, 8, 10 and 11 in Table S4. Figure 2b, entries 1-3 in the article was obtained based on entries 4, 5 and 6 in Table S5.

We calculated carbon balances for the reactions in Table S5 based on ethanol and methanol, respectively. Carbon balance calculated based on ethanol:

$$C_{EtOH} = \frac{\text{ethanol needed to produce 2a}-\text{2f}}{\text{reacted ethanol}}$$

The amount of reacted ethanol and (2a-2f) could all be obtained from GC or HPLC determination. Total amount of ethanol needed to produce (2a-2f) could be calculated from each chemical equation. For example, 1 ethanol molecule and 2 methanol molecules are needed to generate 1 isobutanol molecule, and 2 ethanol molecules are needed to form 1 n-butanol molecule. Carbon balances based on ethanol in Table S5 varied from 89-103%.

Carbon balance calculated based on methanol:

$$C_{MeOH} = \frac{\text{methanol needed to produce 2a}-\text{2e and formic acid}}{\text{reacted methanol}}$$

The amount of reacted methanol and formic acid could also be obtained from quantified determination and the carbon balances based on methanol could be calculated thereof. The concentration of formic acid was no higher than acetic acid after the reaction. Carbon balances based on methanol in Table S5 varied from 87-101%.

Table S4. Catalytic reactions using different Ir catalysts.

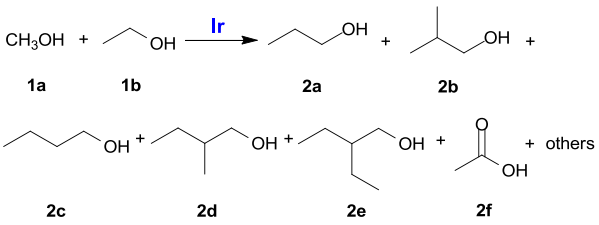

Entry	Catalyst	Conv. **1b** (%)	Selectivity (%)						
			Cross condensation		Self-condensation			**2f**	others [g]
			2a	**2b**	**2c**	**2d**	**2e**		
1	$Ir(acac)_3$-Phen/AC	39	15	29	19	25	3	8	1
2	$IrCl_3$/S1 (5%-105)	8	31	38	15	10	n.d.	6	n.d.
3	$IrCl_3$/S1 (5%-250)	17	36	47	8	5	n.d.	4	<1
4	$IrCl_3$/S2 (5%-250)	15	31	50	9	5	n.d.	5	n.d.
5	$IrCl_3$/S3 (5%-250)	15	29	44	14	9	n.d.	4	n.d.
6	$IrCl_3$/S4 (5%-250)	20	32	55	4	4	n.d.	5	n.d.
7	$IrCl_3$/S5 (5%-250)	21	31	54	6	5	n.d.	4	n.d.
8	$IrCl_3$/S6 (5%-105)	9	37	40	10	8	n.d.	5	n.d.
9	$IrCl_3$/S6 (5%-200)	14	38	43	7	8	n.d.	4	n.d.
10	$IrCl_3$/S6 (5%-250)	31	30	61	4	2	n.d.	3	n.d.
11	$IrCl_3$/S6 (5%-300)	33	33	37	15	8	3	4	<1
12[a]	$IrCl_3$/S6 (5%-400)	37	29	34	16	11	3	6	1
13	$IrCl_3$/S6 (2.5%-250)	21	37	45	6	7	n.d.	5	n.d.
14	$IrCl_3$/S6 (7.5%-250)	24	30	57	4	2	n.d.	7	n.d.
15[a]	$IrCl_3$/S6 (5%-300)	33	32	39	14	8	3	4	n.d.
16[b]	$IrCl_3$/S6 (5%-250)	8	35	52	5	4	n.d.	4	n.d.
17[c]	$IrCl_3$/S6 (5%-250)	26	29	61	2	4	n.d.	4	n.d.
18	$IrCl_3$/S7 (5%-105)	10	35	42	9	9	n.d.	5	n.d.
19	$IrCl_3$/S7 (5%-200)	15	39	43	7	7	n.d.	4	n.d.
20	$IrCl_3$/S7 (5%-250)	32	29	61	4	3	n.d.	3	n.d.
21	$IrCl_3$/S7 (5%-300)	34	32	38	14	8	3	4	1
22[a]	$IrCl_3$/S7 (5%-400)	35	30	36	15	11	2	5	1
23	$IrCl_3$/S8 (5%-250)	27	29	60	3	3	n.d.	5	n.d.
24	$IrCl_3$/S9 (5%-200)	14	35	48	6	7	n.d.	4	n.d.
25	$IrCl_3$/S9 (5%-250)	31	29	61	4	3	n.d.	3	n.d.
26	$IrCl_3$/S9 (5%-300)	34	31	41	11	9	3	5	<1
27	$IrCl_3$/S10 (5%-200)	10	32	51	7	5	n.d.	5	n.d.
28	$IrCl_3$/S10 (5%-250)	32	23	66	4	3	n.d.	4	n.d.
29	$IrCl_3$/S10 (5%-300)	35	27	38	15	11	3	5	<1
30	$IrCl_3$/S11 (5%-250)	29	28	59	5	3	n.d.	5	n.d.
31	Ir/C (5%-250)	16	29	32	18	13	2	6	n.d.

32[d]	$IrCl_3$/S0 (5%-250)	15	31	33	16	13	1	6	n.d.
33[e]	$IrCl_3$/S0 (5%-250)	9	29	30	18	14	3	6	n.d.
34[f]	$IrCl_3$/S6 (5%-300)	19	33	34	16	10	3	4	n.d.
35	no Ir catalyst	0	n.d.	n.d.	n.d.	n.d.	n.d.	n.d.	n.d.
36	Only S6	0	n.d.	n.d.	n.d.	n.d.	n.d.	n.d.	n.d.

Reaction conditions: 1.05 g methanol (32.8 mmol), 0.5 g ethanol (10.9 mmol), 0.44 g NaOH (1 equivalent with respect to ethanol), 0.1 g Ir catalyst and H_2O (10 mL) were mixed together in an autoclave without exclusion of air. The mixture was heated to 160 °C for 16 h under magnetic stirring. Abbreviations of Ir catalysts were as described above. The reactions were quantified analyzed by GC. "n.d." means no detectable. Selectivity of product *i* was calculated based on: (mass amount of product *i*)/ (mass amount of all products). [a]. The catalyst was prepared by calcination under N_2 first and then oxidized at 250 °C in air. [b]. The reaction was carried out under N_2 atmosphere. [c]. 2.1 g methanol, 1.0 g ethanol, 0.88 g NaOH, 0.1 g Ir catalyst and H_2O (10 mL) were reacted at 160 °C for 16 h under air. [d]. The catalyst was prepared by using the pure carbon as the support without N-doping operation. [e]. The catalyst was calcinated in N_2 at 250 °C. [f]. The catalyst was calcinated at 300 °C in N_2. [g]. Small amount of formic acid derived from the oxidation of methanol was also detected in GC, but it was not the product derived from ethanol conversion. The concentration of formic acid was similar to acetic acid.

Table S5. Optimizations of reaction conditions.

Entry	Base	**1a : 1b** (molar ratio)	t (h)	Conv. **1b** (%)	Selectivity (%)						Overall amount (**2a-2f**)	Reacted **1a**
					2a	**2b**	**2c**	**2d**	**2e**	**2f**		
1[a]	LiOH	3:1	16	31	32	58	4	3	n.d.	3	0.21 g	0.16 g
2[a]	K_3PO_4	3:1	16	32	31	60	5	3	n.d.	1	0.22 g	0.17 g
3[a]	K_2CO_3	3:1	16	29	36	55	3	4	n.d.	2	0.20 g	0.16 g
4[b]	NaOH	6:1	32	59	6	85	2	2	n.d.	5	0.43 g	0.34 g
5[b]	K_3PO_4	6:1	32	52	5	91	2	1	n.d.	1	0.38 g	0.33 g
6[b]	K_3PO_4	2:1	32	57	20	70	4	4	n.d.	2	0.38 g	0.29 g
7[c]	K_3PO_4	3:1	16	35	34	59	4	2	n.d.	1	0.22 g	0.17 g
8[d]	K_3PO_4	6:1	32	53	6	90	2	1	n.d.	1	0.42 g	0.38 g

Reaction conditions: methanol, 0.5 g ethanol, 1 equivalent of base with respect to ethanol, Ir catalyst and 10 mL H_2O were reacted at 160 °C. Other conditions were as specified in Table S4. The reactions were quantified analyzed by both GC and HPLC, and the obtained results were within experimental error. [a]. 0.1 g $IrCl_3$/S6 (5%-250) was used. [b]. 0.2 g $IrCl_3$/S6 (5%-250) was used. [c]. 0.1 g $IrCl_3$/S6 (5%-250) and 1.5 equivalents of K_3PO_4 were used. [d]. 0.2 g $IrCl_3$/S10 (5%-250) was used.

Catalytic reactions of ethanol fermentation broth

Ethanol fermentation broth was obtained from Qingdao Institute of Bioenergy and Bioprocess Technology (QIBEBT), Chinese Academy of Sciences. Details about the generation of broth had been published before.[35] The biomass source is inulin and the enzyme catalyst is *S. cerevisiae* strain JZ1C. Industrial broth sample was obtained from Longlive Bio-technology Co., Ltd..

Microbial cells, its debris and other solids could be separated by centrifugation (9000 r/min, 5-10 min). Detailed decolourization procedure: To a 100 mL of flask, 50 mL of the centrifuged yellow fermentation broth and 1.0 g of activated carbon (Vulcan XC72R, Cabot Co., Ltd.) were added. The mixture were stirred at room temperature for 1 h. After that, the mixture was separated by filtration to get the yellowish clear solution (Figure S5).

Concentrations of ethanol and other organic biogenic impurities in the fermentation broth (QIBEBT) were listed in Table S6. Ethanol almost remained the same concentration during the decolourization treatment. As the main detectable byproducts, glycerol was adsorbed by activated carbon. Ethanol concentration in the fermentation broth obtained from industrial company (Longlive Bio-technology Co., Ltd.) was a little lower (45.3 mg/mL).

Table S6. The concentration of organic components in fermentation broth before and after decolourization.

Component	Concentration (mg/mL)	
	Before decolourization	After decolourization
Ethanol	95.5	95.3
Glycerol	5.3	2.0
Acetic acid	0.7	0.3
Methanol	0.2	0.16
Propanol	0.2	0.18

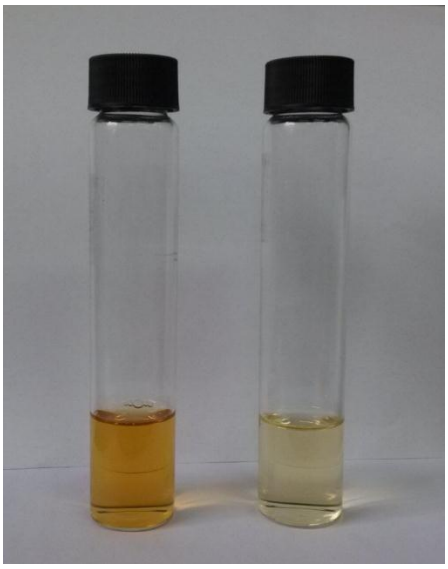

Figure S5. Photos of bio-ethanol fermentation broth. Left: yellow solution after centrifugation to separate yeast. Right: yellowish solution after centrifugation and decolourization using activated carbon.

Table S7. Reactions of methanol with ethanol fermentation broth.

Entry	**1a : 1b** (molar ratio)	T (°C) - t (h)	Conv. **1b** (%)	Selectivity (%)					
				2a	**2b**	**2c**	**2d**	**2e**	**2f**
1[a]	3:1	160-16	15	43	46	5	3	n.d.	3
2[b]	3:1	160-16	36	33	58	5	2	n.d.	2
3[b]	6:1	160-32	49	5	90	2	1	n.d.	2
4[c]	3:1	160-16	35	31	60	4	3	n.d.	2

Reaction conditions: methanol, 5 mL ethanol fermentation broth (QIBEBT), 0.2 g catalyst $IrCl_3$/S6 (5%-250) and 2.8 g K_3PO_4 $3H_2O$ in 5 mL H_2O were reacted in an autoclave without exclusion of air. Other conditions were as specified in Table S6. The reactions were quantified analyzed by both GC and HPLC, and the obtained results were within experimental error. [a]. Bio-ethanol fermentation broth after centrifugation treatment was used. [b]. Bio-ethanol fermentation broth after centrifugation and decolourization treatments was used. [c]. Bio-ethanol fermentation broth (Longlive Bio-technology Co., Ltd.) after centrifugation and decolourization treatments was used.

In addition, there are other organic components existed in the fermentation broth which contributed to the yellow color. However, these color components were not detectable by GC or HPLC. Color compositions might derive from the seed and fermentation medium such as peptone, yeast extract and biomass feedstock. Experimental results suggested they were harmful to the reaction rate (Table S7, entry 1). However, a simple decolourization treatment

using activated carbon could reduce this negative influence. Ethanol conversion, selectivity to isobutanol and overall cross condensation products were generally identical to the reactions of pure methanol and ethanol mixture under optimized conditions (Table S7, entry 3).

Figure 2b, entry 4 in the article was obtained based on entry 3 in Table S7.

IR (Infrared spectroscopy) and UV-Vis (Ultraviolet Visible spectrometry) were used to detect the color components further. IR was detected on Thermo scientific Nicolet iN 10 IR Microscope by the KBr pellet pressing method. UV-Vis was recorded on Perkin-Elmer Lambda 25 Spectrometer with the wavelength ranging from 200 to 700 nm.

Activated carbon used in the decolourization was separated and dried in the oven. IR was used to detect any differences of chemical groups adsorbed on the carbon materials before and after decolourization. But there were no characteristic adsorption peaks both in the used and pristine carbon materials (Figure S6).

During the UV-Vis analysis, both the pristine and decoloured fermentation broth were diluted to 6 times using deionized water, and deionized water was used as the blank sample for the correction of background. Absorbance data were reported in the wavelength range from 200 to 700 nanometers (nm). Figure S7 indicated that both samples had absorbance maxima (λ_{max}) at approximately 325 nm. The pristine broth exhibited greater absorbance than the decolored broth, with the absorbance value of 1.8008 and 0.3403 respectively. The decolourization ratio was 81.1% as calculated by the following Equation 1 (η% was the decolourization ratio, A_0 was the absorbance value of the pristine fermentation broth, A was the absorbance value of the decoloured fermentation broth).

$$\eta\% = \frac{A_0 - A}{A_0} \times 100\% \quad \text{.....Equation 1.}$$

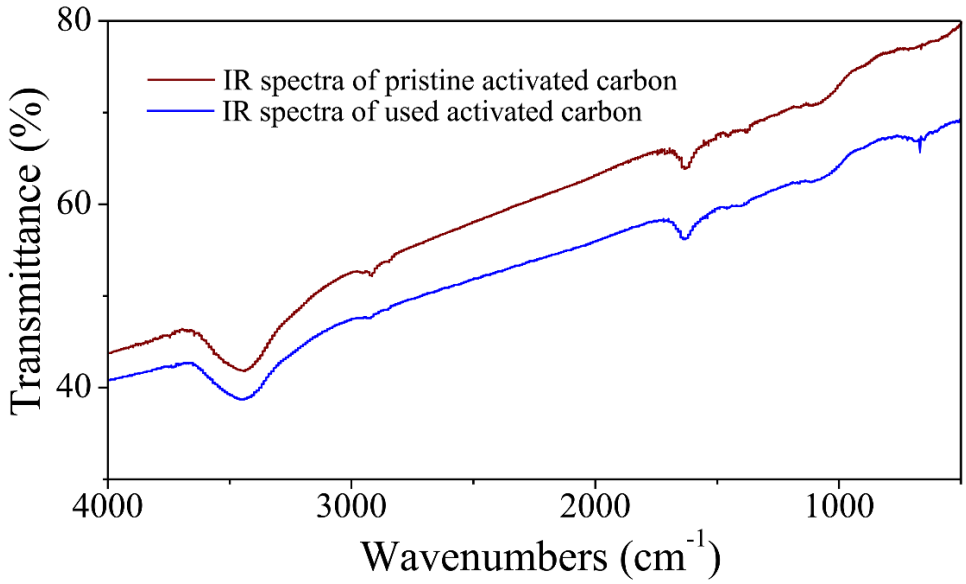

Figure S6. IR spectra of pristine carbon material and separated carbon material used in decolourization.

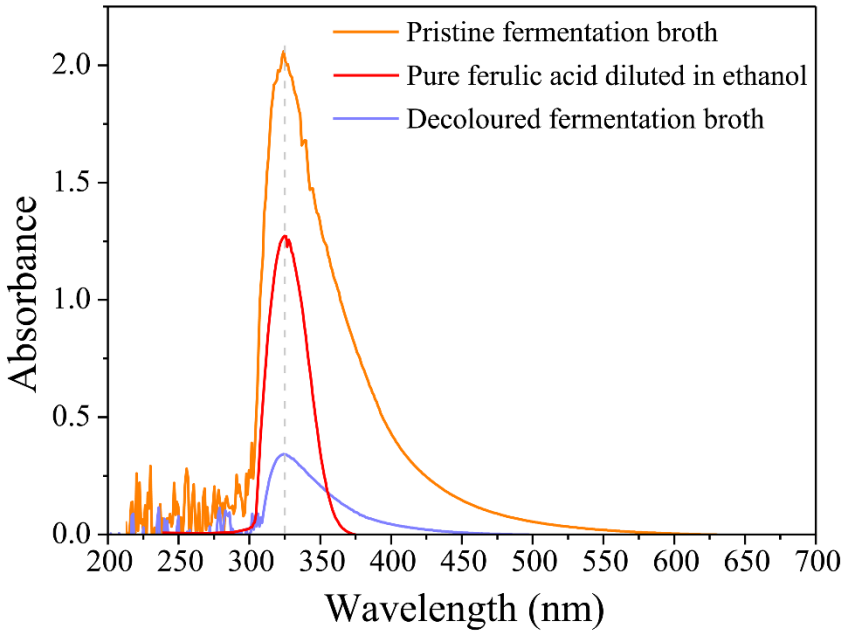

Figure S7. UV-Vis spectra of the decoloured and pristine fermentation broth.

According to the reference, phenolic acids such as chlorogenic acids, caffeic acid and ferulic acid are generally found in UV-Vis spectrum with a maximum absorption peak at 325 nm.[36] Ferulic acid and its sugar ester have high antioxidative activity with a methoxy group for the characteristic absorption peak at 325 nm in UV-Vis spectrum. In addition, ferulic acid was found to play significant role in cell wall extensibility and its growth. Ferulic acid was identified

as one of the inhibitors derived from lignocellulosic biomass during ABE fermentation for butanol production. High concentration of ferulic acid was contained in the hydrolyzed solution of inulin based Jerusalem artichoke, which was harmful for bacteria growth and butanol production.[37] Considering these references and the fact that our used fermentation broth was obtained by the bio-conversion of inulin, we proposed that the ferulic acid or its derivatives were the main color components in the fermentation broth.

Control experiments were carried out in the presence of glycerol and ferulic acid under otherwise identical conditions. Pure ferulic acid was added to ethanol solution to obtain similar absorbance value with respect to the pristine fermentation broth. Experimental results confirmed obvious inhibiting effect of ferulic acid on condensation reaction, while glycerol in this concentration didn't influence the condensation obviously (Table S8).

Table S8. Control experiments in the presence of glycerol and ferulic acid.

Entry	Additive	Conv.**1b** (%)	Selectivity (%)						TOF (h^{-1})
			2a	**2b**	**2c**	**2d**	**2e**	**2f**	
1	/	28	32	62	4	1	n.d.	1	46.8
2[a]	Glycerol	26	32	61	5	1	n.d.	1	43.5
3[b]	Ferulic acid	11	32	58	6	3	n.d.	1	18.4

Reaction conditions: 0.5 g of ethanol, 6 equivalents of methanol with respect to ethanol, 1 equivalent of K_3PO_4 with respect to ethanol, 0.1 g Ir catalyst $IrCl_3$/S6 (5%-250) and H_2O (10 mL) were mixed together in an autoclave without exclusion of air. The mixture was heated to 160 °C for 10 h under magnetic stirring. "n.d." means no detectable. [a]. 0.025 g of glycerol was added. [b]. 0.035g of ferulic acid was added.

Recycling and time-resolved experiments

After cooling down to room temperature, the catalyst was isolated from the reaction mixture by filtration and then dried at 105 °C under air atmosphere. According to the Ir 4f XPS spectra, about 76% of Ir was reduced to lower oxidation state (Figure S8). So that a similar oxidation treatment (250 °C-8h, air) was applied to regenerate active Ir catalyst with higher oxidation state. The separated catalyst was also dried under vacuum at room temperature for comparison. XPS spectra indicated the content of Ir with different oxidation state were generally the same (Figure S9). Ir with lower oxidation state all exceeded 70%. Ir particles were resistant to be further oxidized at the temperature of 105 °C. A higher temperature oxidation (250 °C) is necessary to obtain Ir catalyst with higher oxidation state.

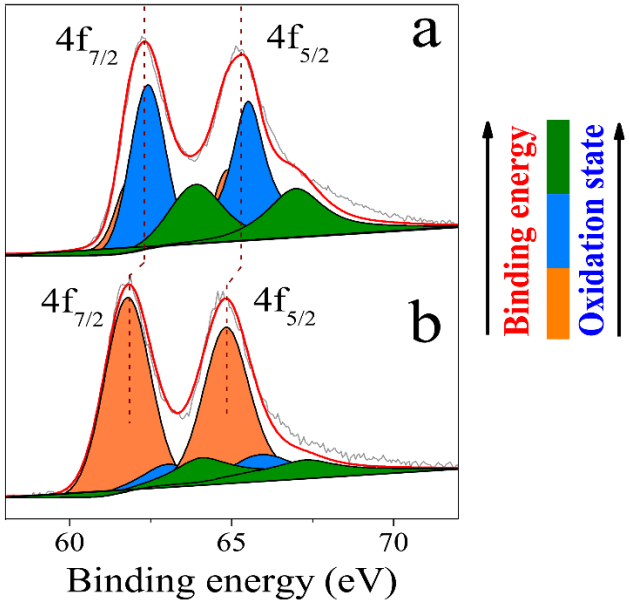

Figure S8. Ir 4f XPS of spectra of Ir catalysts before and after the reaction. a: fresh catalyst $IrCl_3$/S6 (5%-250); b: isolated catalyst $IrCl_3$/S6 (5%-250).

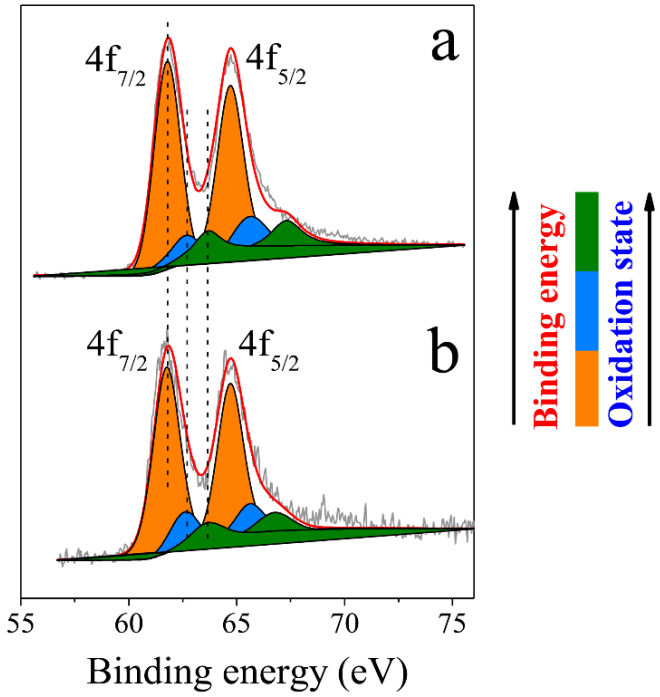

Figure S9. Ir 4f XPS spectra of separated Ir catalysts. a, the catalyst was dried at 105 °C under air; b, the catalyst was dried under vacuum at room temperature.

Time-resolved experiments were performed under the same conditions except the reaction time ranged from 2, 6, 10, to 16 h (Table S9). XPS were used to characterize the oxidation state of each separated Ir catalysts in order to obtain more information about the changing process of oxidized Ir. Importantly, XPS results indicated that the four isolated Ir catalysts were all reduced to the same degree (Figure S10). While the TON (turnover number) and ethanol conversion were all continuously increased with reaction time. The distribution of cross-condensation products exceeded 90% even at 2 hours reaction time.

Considering that reduced Ir catalyst exhibited very low conversion and uncontrolled selectivity toward cross-condensation, the results from time resolved experiments indicated that active oxidized Ir could be regenerated during the transformation. The oxidized Ir was reduced when isolated from the reaction system.

Reaction procedures using the recycled catalyst were the same as the reactions using fresh catalyst. After five runs, the catalyst still gave 33% of ethanol conversion (80% of the conversion in the first run, Table S10) and always good selectivity to cross condensation products. The particle size did not changed significantly under hydrothermal basic conditions. Both TEM and XRD confirmed that Ir catalyst still remained highly dispersed (mainly 1-2 nm)

under hydrothermal basic conditions. Even after 5 cycles, Ir particles exhibited good stability against aggregation and the particle size only changed slightly (Figures S11, S12).

Table S9 Results of time-resolved experiments.

Entry	t (h)	Conv.**1b** (%)	Selectivity (%)						TOF (h^{-1})	TON
			2a	**2b**	**2c**	**2d**	**2e**	**2f**		
1	2	10	36	56	6	2	n.d.	n.d.	83.6	167.2
2	6	21	32	60	4	2	n.d.	2	58.5	351.0
3	10	28	32	62	4	1	n.d.	1	46.8	468.0
4	16	37	30	65	3	1	n.d.	1	38.7	619.2

Reaction conditions: 0.5 g ethanol, 6 equivalents of methanol with respect to ethanol, 1 equivalent of K_3PO_4 with respect to ethanol, 0.1 g Ir catalyst $IrCl_3$/S6 (5%-250) and H_2O (10 mL) were mixed together in an autoclave without exclusion of air. The mixture was heated to 160 °C for the reaction time under magnetic stirring. "n.d." means no detectable.

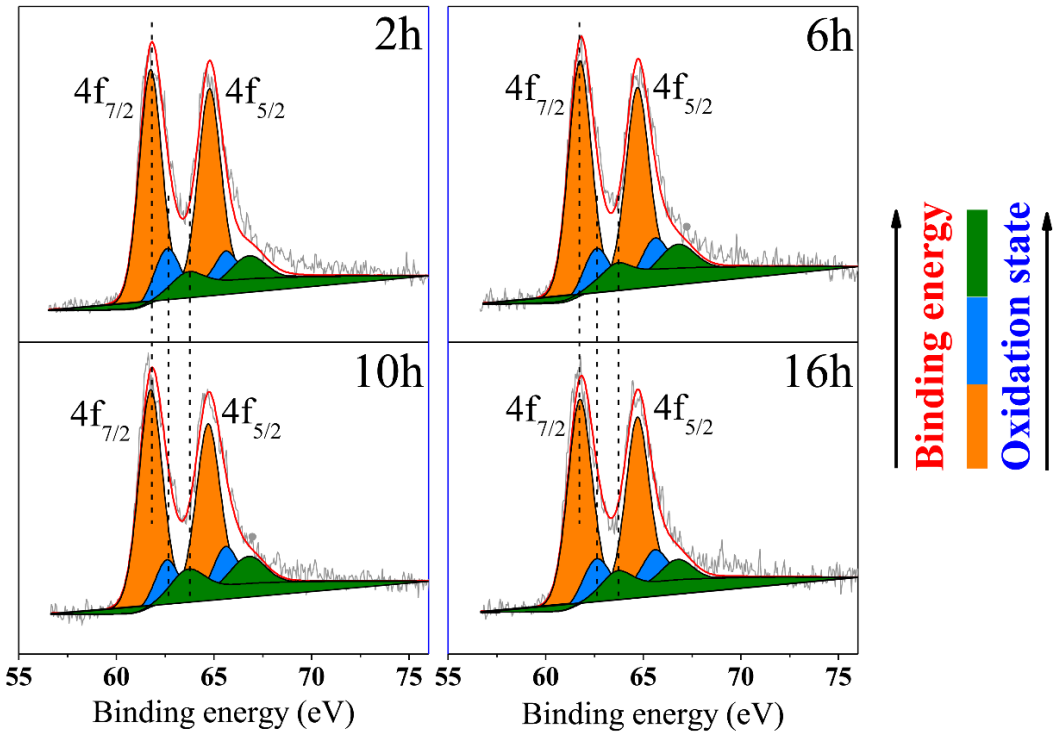

Figure S10. Ir 4f spectra of the separated catalysts after the reaction of 2, 6, 10, 16 h.

Table S10. Reactions of methanol with ethanol using the recycled catalyst.

Entry	Conv. **1b** (%)	Selectivity (%)					
		Cross condensation		Self-condensation			**2f**
		2a	**2b**	**2c**	**2d**	**2e**	
1st run	41	25	67	5	2	n.d.	1
2nd run	39	23	68	5	2	n.d.	2
3rd run	35	26	65	5	3	n.d.	1
4th run	35	24	67	5	3	n.d.	1
5th run	33	29	63	5	2	n.d.	1

Reaction conditions: 1.05 g methanol (32.8 mmol), 0.5 g ethanol (10.9 mmol), 2.9 g $K_3PO_4 \cdot 3H_2O$ (10.9 mmol, 1 equivalent with respect to ethanol), 0.2 g recycled $IrCl_3$/S6 (5%-250) catalyst and H_2O (10 mL) were mixed together in an autoclave without exclusion of air. The mixture was heated to 160 °C for 16 h under magnetic stirring. The reactions were quantified analyzed by GC.

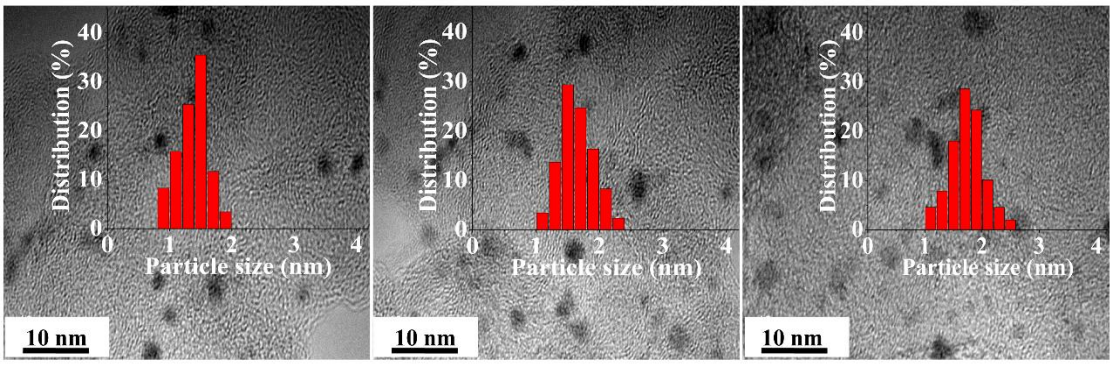

Figure S11. HRTEM images and particle size distributions of fresh catalyst (left), two-times used catalyst (middle) and five-times used catalyst (right).

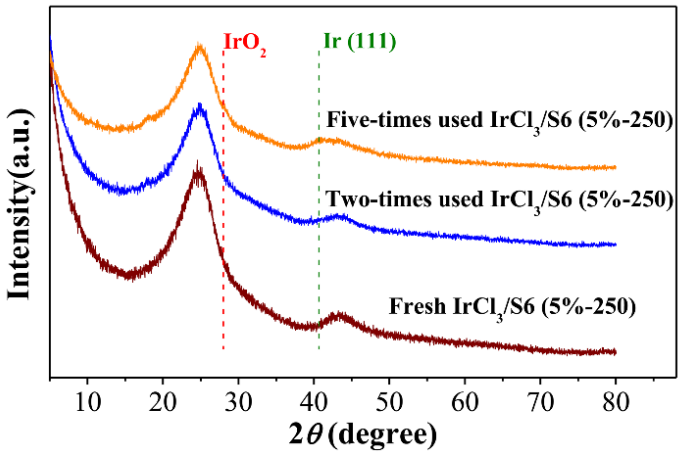

Figure S12. XRD patterns of fresh and separated Ir catalysts.

The interaction of N-groups with Ir was also evidenced from the XPS analyses of $IrCl_3$/S0 (5%-250) and $IrCl_3$/S6 (5%-250) (Figure S13). Ir 4f spectra shifted to higher binding energy (about 0.6 eV) due to the coordination or interaction N groups.[34] The dispersion of Ir on supports S0 and S6 were also different as indicated above in CO pulse chemisorption (Table S3).

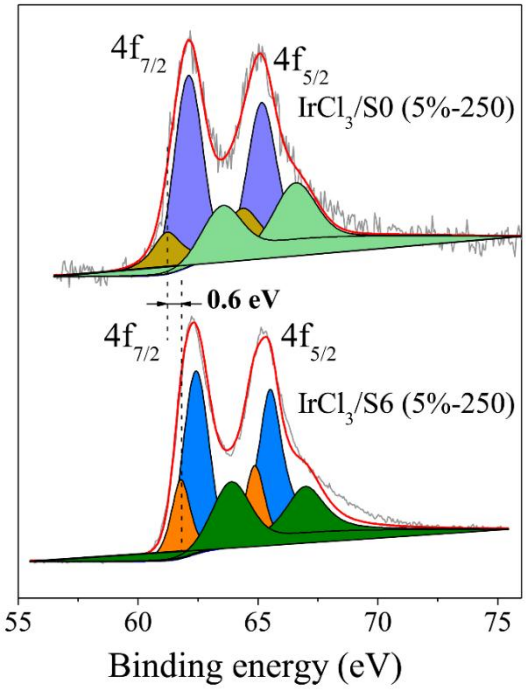

Figure S13. Ir 4f XPS spectra of Ir catalysts prepared using N-functionalized support and pristine carbon material.

Control experiments using reaction intermediates

Reactions of methanol with propanol

Reaction procedures: methanol (0.32 g, 10 mmol), propanol (0.6 g, 10 mmol), $K_3PO_4 \cdot 3H_2O$ (2.6 g, 10 mmol), 0.1 g Ir catalyst and H_2O (10 mL) were reacted at 160 °C for 16 h under air atmosphere. Reaction products were analyzed using GC and the products' distributions were listed in Figure S14.

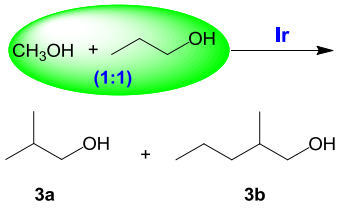

Catalyst	Mass ratio (**3a : 3b**)
$IrCl_3$/S6 (5%-250)	15.2 : 1
$Ir(acac)_3$-Phen/AC	1.2 : 1
$IrCl_3$/S6 (5%-300)	2.3 : 1

Figure S14. Products' distributions in the condensation of methanol with propanol.

Reactions of methanol with ethanol and acetaldehyde mixture

Reaction procedures: methanol (1.05 g, 32.8 mmol), ethanol (0.36 g, 7.8 mmol), acetaldehyde solution (0.50 g, 35 wt%, 4.0 mmol), $K_3PO_4 \cdot 3H_2O$ (3.1 g, 11.6 mmol), 0.2 g catalyst $IrCl_3$/S6 (5%-250) and H_2O (10 mL) were mixed together in an autoclave without exclusion of air. The mixture was heated to 160 °C for 16 h under magnetic stirring. Products were quantified analyzed by GC.

For comparison, the reaction without Ir catalyst was carried out under otherwise identical conditions. Reaction solution was analyzed using GC and GC-MS. Solid product was weighed in balance. Elemental analysis indicated 76.6 % C and 4.5% H content in this yellow brown solid.

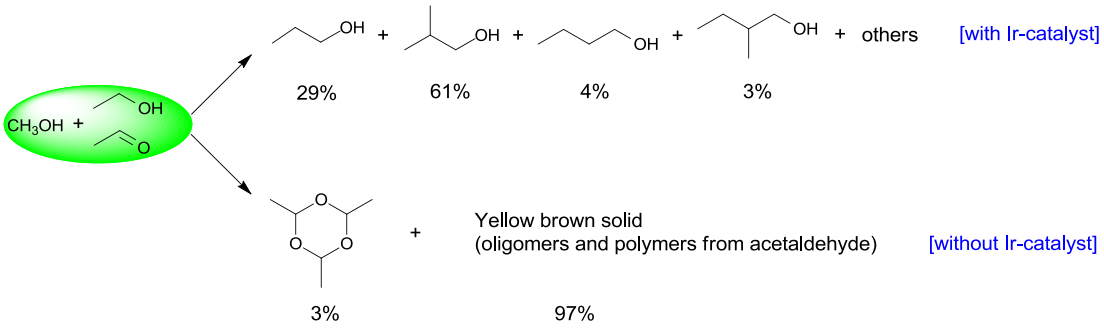

Figure S15. Reactions of methanol with ethanol and acetaldehyde mixture.

Reaction products' distribution was unchanged and cross condensation pathway still exhibited overwhelming selectivity in the presence of Ir catalyst $IrCl_3$/S6 (5%-250). Side products derived from the self-aldol reaction of acetaldehyde were suppressed by Ir catalyst. In comparison, without Ir catalyst, base catalyzed aldol reaction of acetaldehyde generated lots of side products (*e.g.* yellow brown solid oligomers and polymers) and there were no higher alcohols formed (Figure S15).